

Quick iterative scheme for the calculation of transfer matrices: application to Mo (100)

This content has been downloaded from IOPscience. Please scroll down to see the full text.

1984 J. Phys. F: Met. Phys. 14 1205

(<http://iopscience.iop.org/0305-4608/14/5/016>)

View [the table of contents for this issue](#), or go to the [journal homepage](#) for more

Download details:

IP Address: 18.140.1.248

This content was downloaded on 06/04/2015 at 21:46

Please note that [terms and conditions apply](#).

Quick iterative scheme for the calculation of transfer matrices: application to Mo(100)

M P López Sancho, J M López Sancho and J Rubio

Instituto de Física de Materiales, CSIC, Serrano 144, Madrid 6, Spain

Received 14 September 1983

Abstract. The transfer matrix of a solid described by the stacking of principal layers is obtained by an iterative procedure which takes into account 2^n layers after n iterations, in contrast to usual schemes where each iteration includes just one more layer. The Green function and density of states at the surface of the corresponding semi-infinite crystal are then given by well known formulae in terms of the transfer matrix.

This method, especially convenient near singularities, is applied to the calculation of the spectral as well as the total densities of states for the (100) face of molybdenum. The Slater–Koster algorithm for the calculation of tight-binding parameters is used with a basis of nine orbitals per atom (4d, 5s, 5p). Surface states and resonances are first identified and then analysed into orbital components to find their dominant symmetry. Their evolution along the main symmetry lines of the two-dimensional Brillouin zone is given explicitly. The surface-state peak just below the Fermi level (Swanson hump) is not obtained. This is traced to the difficulty in placing an appropriate boundary condition at the surface with the tight-binding parametrisation scheme.

1. Introduction

Iterative methods for the calculation of the Green function at the surface layer of a solid (Haydock *et al* 1972, Ainschchik *et al* 1976, Foo *et al* 1976, Mele and Joannopoulos 1978) have sometimes been criticised on the basis of convergence arguments (Dy *et al* 1979, Lee and Joannopoulos 1981a, b). Thus the ‘effective field’ or transfer-matrix approach gives the surface (zeroth-layer) Green function by the equation

$$G_{00}(\omega) = (\omega - H_{00} - H_{01} T(\omega))^{-1} \quad (1)$$

where H_{00} and H_{01} are matrix elements of the Hamiltonian between layer Bloch states (see below) and the transfer matrix T is given by

$$T(\omega) = (\omega - H_{00} - H_{01} T(\omega))^{-1} H_{01}^* \quad (2)$$

which must be calculated by iterating until self-consistency is achieved. This usually involves many iterations (an average of ~ 50), especially in the neighbourhood of the singularities of $G(\omega)$ where several hundred may be needed to get an accurate result.

In this paper we propose a new iterative scheme for the calculation of the transfer matrix which converges very quickly. After n iterations 2^n layers are taken into account instead of the n layers one would have included with the usual method based on iterating equation (2). Away from singularities, five or six iterations usually suffice to get a convergent result ($2^5 = 32$, $2^6 = 64$ with equation (2)). Close to singularities, the number of

iterations increases up to 14 or 15, i.e., about twice those needed at regular points; to get the same accuracy with equation (2) one would need 16384 or 32768 iterations, i.e., five hundred times those needed at regular points. Thus, it is just close to singularities, when the usual scheme converges very slowly, where the new scheme becomes more convenient, saving a considerable amount of computing time. In fact, the closer to singularities we are, the greater the advantage the new scheme offers over the usual one†.

The iterative scheme is presented in § 2, followed in § 3 by little more than a recollection of the formulae to be used. Section 4 analyses the spectral and total densities of states for the (100) surface of molybdenum. The calculation does not give the surface-state peak (Swanson hump). Some concluding remarks are offered in § 5, particularly in connection with the Swanson hump and surface boundary conditions.

2. Iterative scheme

As is well known (Lee and Joannopoulos 1981a), any solid with a surface can be described by a semi-infinite stack of principal layers. A principal layer is defined as the smallest group of neighbouring atomic planes such that only nearest-neighbour interactions exist between principal layers. If the bulk periodicity parallel to the surface is preserved by all the atomic planes right up to the surface, then k_{\parallel} is a good quantum number. For each k_{\parallel} , the surface problem reduces to a one-dimensional chain in the direction (z) perpendicular to the surface. To this end we build Bloch-state orbitals for each atomic orbital φ_{α} along any atomic plane, for example the λ th atomic plane of the n th principal layer. Take m orbitals per atom and suppose each principal layer is composed of l atomic planes. Then one can form column-vector Bloch states for each principal layer

$$\Psi_n(k_{\parallel}) = \begin{pmatrix} \varphi_n^{1l}(k_{\parallel}) \\ \vdots \\ \varphi_n^{\lambda\alpha}(k_{\parallel}) \\ \vdots \\ \varphi_n^{im}(k_{\parallel}) \end{pmatrix} \quad (3)$$

where

$$\varphi_n^{\lambda\alpha}(k_{\parallel}) = \frac{1}{\sqrt{N_{\parallel}}} \sum_{\mathbf{R}_{\parallel}} \exp(i\mathbf{k}_{\parallel} \cdot \mathbf{R}_{\parallel}) \varphi_n^{\lambda\alpha}(\mathbf{R}_{\parallel}). \quad (4)$$

N_{\parallel} and \mathbf{R}_{\parallel} denote numbers of atoms and lattice vectors of an atomic plane. Taking matrix elements of $(\omega - H)G = \mathbf{I}$ between the Bloch states (4), one has the usual chain of equations for the matrix elements of the Green function with fixed k_{\parallel}

$$\begin{aligned} (\omega - H_{00})G_{00} &= \mathbf{I} + H_{01}G_{10} \\ (\omega - H_{00})G_{10} &= H_{01}^{\dagger}G_{00} + H_{01}G_{20} \\ &\vdots \\ (\omega - H_{00})G_{n0} &= H_{01}^{\dagger}G_{n-1,0} + H_{01}G_{n+1,0} \end{aligned} \quad (5)$$

† Note, of course, that no expansion whatever may be made to converge right at a singularity. A small imaginary part must always be added to the energy in order to calculate Green functions, T matrices, etc.

where $n = 0$ denotes the surface principal layer and the matrices

$$\begin{aligned}
 H_{nn'}(\mathbf{k}_{\parallel}) &= \langle \Psi_n(\mathbf{k}_{\parallel}) | H | \Psi_{n'}(\mathbf{k}_{\parallel}) \rangle \\
 G_{nn'}(\omega, \mathbf{k}_{\parallel}) &= \langle \Psi_n(\mathbf{k}_{\parallel}) | G(\omega) | \Psi_{n'}(\mathbf{k}_{\parallel}) \rangle
 \end{aligned}
 \tag{6}$$

and I (the unit matrix) are of rank $l \times m$. In equation (5) we have made the simplifying but not essential assumption of an ideal surface, i.e., $H_{00} = H_{11} = \dots$ and $H_{01} = H_{12} = \dots$. Now we are in a position to discuss our iterative scheme for the calculation of the transfer matrix.

The general term in equation (5) can be rewritten as

$$G_{n0} = (\omega - H_{00})^{-1} (H_{01}^+ G_{n-1,0} + H_{01} G_{n+1,0}) = t_0 G_{n-1,0} + \tilde{t}_0 G_{n+1,0} \quad (n \geq 1) \tag{7}$$

where, clearly,

$$\begin{aligned}
 t_0 &= (\omega - H_{00})^{-1} H_{01}^+ \\
 \tilde{t}_0 &= (\omega - H_{00})^{-1} H_{01}.
 \end{aligned}
 \tag{8}$$

Applying equation (7) again to G_{n-10} and G_{n+10} , we have

$$G_{n0} = t_0(t_0 G_{n-2,0} + \tilde{t}_0 G_{n0}) + \tilde{t}_0(t_0 G_{n0} + \tilde{t}_0 G_{n+2,0}),$$

i.e.,

$$G_{n0} = t_1 G_{n-2,0} + \tilde{t}_1 G_{n+2,0} \quad (n \geq 2), \tag{9}$$

with

$$\begin{aligned}
 t_1 &= (I - t_0 \tilde{t}_0 - \tilde{t}_0 t_0)^{-1} t_0^2 \\
 \tilde{t}_1 &= (I - t_0 \tilde{t}_0 - \tilde{t}_0 t_0)^{-1} \tilde{t}_0^2.
 \end{aligned}
 \tag{10}$$

Since equation (9) is isomorphic to equation (7), the process can be repeated iteratively. After i iterations

$$G_{n0} = t_i G_{n-2^i,0} + \tilde{t}_i G_{n+2^i,0} \quad n \geq 2^i \tag{11}$$

where

$$\begin{aligned}
 t_i &= (I - t_{i-1} \tilde{t}_{i-1} - \tilde{t}_{i-1} t_{i-1})^{-1} t_{i-1}^2 \\
 \tilde{t}_i &= (I - t_{i-1} \tilde{t}_{i-1} - \tilde{t}_{i-1} t_{i-1})^{-1} \tilde{t}_{i-1}^2
 \end{aligned}
 \tag{12}$$

are at least of order 2^i in H_{01} . Letting $n = 2^i$ in equation (11), the following chain of equations is obtained:

$$\begin{aligned}
 G_{10} &= t_0 G_{00} + \tilde{t}_0 G_{20} \\
 G_{20} &= t_1 G_{00} + \tilde{t}_1 G_{40} \\
 &\vdots \\
 G_{2^{n0}} &= t_n G_{00} + \tilde{t}_n G_{2^{n+10}}
 \end{aligned}
 \tag{13}$$

where

$$\begin{aligned}
 G_{10} &= t_0 G_{00} + \tilde{t}_0 G_{20} \\
 &= (t_0 + \tilde{t}_0 t_1) G_{00} + \tilde{t}_1 G_{40} \\
 &= (t_0 + \tilde{t}_0 t_1 + \tilde{t}_0 \tilde{t}_1 t_2) G_{00} + \tilde{t}_2 G_{80} \\
 &= (t_0 + \tilde{t}_0 t_1 + \dots + \tilde{t}_0 \dots \tilde{t}_{n-1} t_n) G_{00} + \tilde{t}_n G_{2^{n+1}0}.
 \end{aligned} \tag{14}$$

The process is to be repeated until $t_{n+1}, \tilde{t}_{n+1} < \epsilon$, as small as one wishes; then $G_{2^{n+1}0} \simeq 0$ and the last of equations (13) gives

$$G_{2^{2n}0} = t_n G_{00} \tag{15}$$

or

$$t_n = T^{2^n}$$

which states that the t_n are increasingly better approximations to the 2^n th powers of the transfer matrix. Equation (14) now gives an expansion for T , i.e., $G_{10} = TG_{00}$ with

$$T = t_0 + \tilde{t}_0 t_1 + \tilde{t}_0 \tilde{t}_1 t_2 + \dots + \tilde{t}_0 \dots \tilde{t}_{n-1} t_n \tag{16}$$

where the n th term is of order $2^{n+1} - 1$ in H_{01} and should get vanishingly small quite rapidly; it incorporates the effects of 2^n layers. Thus the first term relates G_{10} directly to G_{00} ; in the second term, \tilde{t}_0 relates G_{10} to G_{20} while t_1 relates G_{20} to G_{00} , i.e., this term relates G_{10} to G_{00} through G_{20} ; similarly, the third term incorporates the effect of G_{20} and G_{40} , and so on.

3. Diagonal matrix elements of G

This section is a simple recollection of well known formulae to be used in the calculation of the spectral density of states for an atomic plane of a given layer. The spectral density of states for the l th atomic plane of the n th layer is given by

$$N_n^l(\mathbf{k}_{\parallel} \epsilon) = -\frac{1}{\pi} \text{Im} \sum_{\alpha} G_{nn}^{l\alpha, l\alpha}(\mathbf{k}_{\parallel} \epsilon + i\eta). \tag{17}$$

$n=0, l=0$ gives, of course, the density of states at the surface.

In what follows we shall be interested in the first four atomic planes of Mo (100). Since interactions will be included up to second-order neighbours only, the principal layers will consist of two atomic planes and, therefore, we need G_{00} and G_{11} .

Once T is known, G_{00} is given trivially by the first of equations (5), i.e.,

$$(\omega - H_{00} - H_{01} T) G_{00} = I \tag{18}$$

or

$$G_{00} = (\omega - H_{00} - H_{01} T)^{-1},$$

which is just equation (1), a well known result given here only for the sake of reference. G_{11} comes out easily by combining the two equations

$$(\omega - H_{00} - H_{01} T) G_{11} = I + H_{01}^* G_{01}$$

$$(\omega - H_{00}) G_{01} = H_{01} G_{11}.$$

One obtains trivially

$$G_{11} = [\omega - H_{00} - H_{01}T - H_{01}^+(\omega - H_{00})^{-1}H_{01}]^{-1}. \quad (19)$$

4. Surface density of states at Mo (100)

We shall take a tight-binding Hamiltonian with a basis of nine orbitals per atom (4d, 5s, 5d) which are assumed to be orthogonal. This Hamiltonian will be parametrised through the Slater-Koster (1954, hereafter referred to as sk) algorithm in the two-centre approximation. The sk parameters have been obtained by fitting to the non-relativistic bulk bands of Petroff and Viswanathan (1971). Some third-order neighbour parameters were needed, but they turned out to be rather small and were put equal to zero in the surface calculation. A list of the sk parameters for Mo is given in table 1.

The principal layers are conveniently formed by two atomic planes. Therefore all the matrices considered in §§ 2 and 3 will be 18×18 matrices. The densities of states at the surface and second atomic plane come from G_{00} , whereas the corresponding quantities at the third and fourth atomic planes come from G_{11} .

Figure 1 shows the spectral density of states at the special points $\bar{\Gamma}$, \bar{X} and \bar{M} of the two-dimensional Brillouin zone (first, second and third columns, respectively) on the surface (row (a)), first, second and third atomic planes (rows (b), (c) and (d), respectively). We find a single peak at the point $\bar{\Gamma}$ (Γ_1), three at the point \bar{X} (X_1 , X_2 and X_3) and two at the point \bar{M} (M_1 and M_2). Table 2 gives the main orbital components of the five peaks, ignoring those with a weight less than 1%. The peak positions are also given in the first row of table 2. Four of these resonances, Γ_1 , X_1 , X_2 and M_1 , are occupied (the Fermi level lies at 0.82 Ryd) and place most of their charge on the surface with a small component on the second atomic plane.

Figures 2, 3 and 4 show the evolution of these resonances along the symmetry lines $\bar{\Gamma}-\bar{X}$ ($\bar{\Delta}$), $\bar{\Gamma}-\bar{M}$ ($\bar{\Sigma}$) and $\bar{X}-\bar{M}$ (\bar{Y}), respectively, shown in the inset at the top left of each figure. Taking, for example, the $\bar{\Delta}$ direction, we see (figure 2) how Γ_1 evolves into Δ_1 to end up as X_1 ; this corresponds to the low-lying band of surface resonances (Weng *et al* 1978) which also extends somewhat (about one third of the way) into the $\bar{\Sigma}$ direction

Table 1. sk parameters (Ryd) obtained through a fit to the bulk band structure of Mo. (The two values for the zeroth-order parameters $(dd)_0^1$ and $(dd)_0^2$ correspond to the irreducible representations t_{2g} and e_{2g} respectively.)

	$(ss)_0 = 1.3652$	$(pp)_0 = 1.7022$ First order	$(dd)_0^1 = 0.8710$ $(dd)_0^2 = 0.8104$ Second order
ss σ	-0.1084		-0.0387
pp σ		0.2004	0.0973
pp π	-0.0506		-0.0093
dd σ	-0.1003		-0.0635
dd π		0.0518	0.0087
dd δ	-0.0052		0.0036
sp σ		0.1460	0.0653
sd σ		0.0982	0.0608
pd σ		0.1992	0.0883
pd π		-0.0281	-0.0101

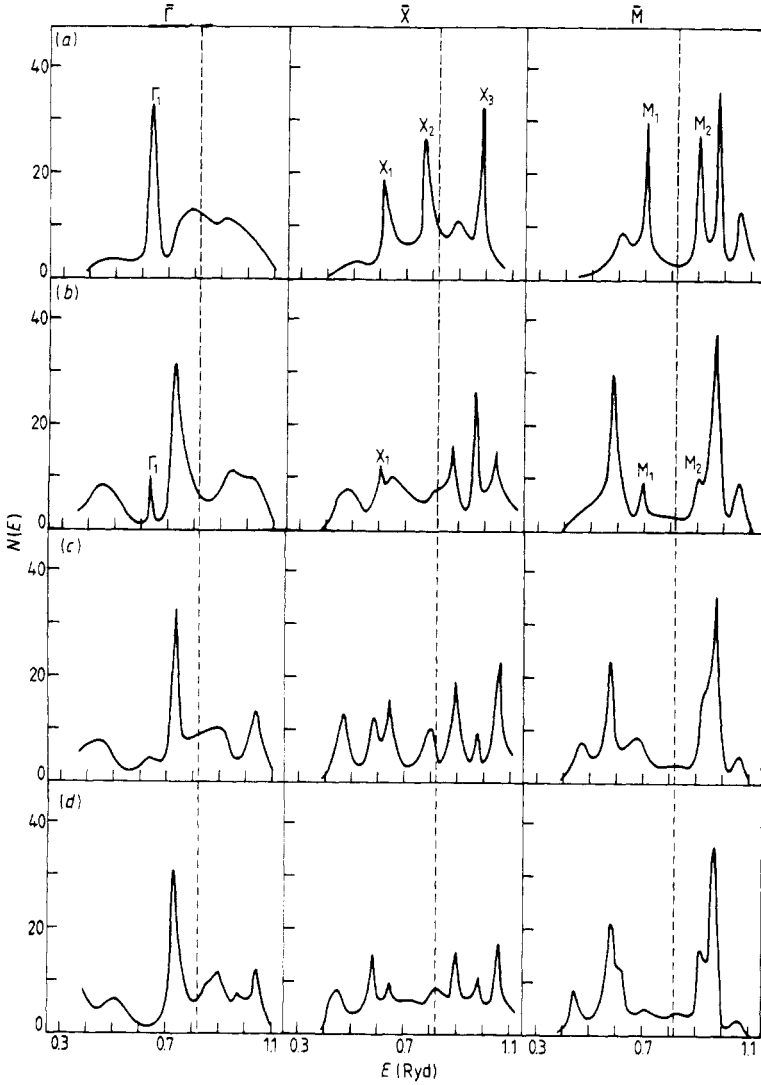


Figure 1. Spectral density of states of Mo(100) at special points $\bar{\Gamma}$, \bar{X} and \bar{M} of the two-dimensional Brillouin zone: (a) for the surface; (b) for the second layer; (c) for the third layer; (d) for the fourth layer. The Fermi level is indicated by the vertical broken lines.

(resonance Σ_1 at the point $(\frac{1}{4}, \frac{1}{4})^\dagger$ in figure 3) as well as into the \bar{Y} direction (resonance Y_1 at the point $(\frac{1}{2}, \frac{3}{8})$ in figure 4).

A second surface band, this time of symmetry Δ_2 , Σ_2 , is found crossed by the Fermi level. It extends all the way along both the $\bar{\Delta}$ and $\bar{\Sigma}$ directions, as well as part of the \bar{Y} direction, but does not exist at the $\bar{\Gamma}$ point. As one moves away from $\bar{\Gamma}$ along, say, the $\bar{\Delta}$ direction (figure 2), a double resonance of symmetry Δ_2 is found. This splits a little further along the way into Δ_2 , which remains occupied, and Δ'_2 , which crosses the Fermi level at about the point $(\frac{1}{4}, 0)$. As the \bar{X} point is approached, both become localised on the surface

† All k vectors are given in units of $2\pi/a$.

Table 2. Orbital composition of main surface resonances.

	Γ_1	X_1	X_2	X_3	M_1	M_2
Energy (Ryd)	0.63	0.65	0.8	0.98	0.7	0.9
$3z^2-r^2$	56.28	43.04	13.76	37.91		92.78
x^2-y^2	19.16	18.01	5.67	25.80		2.05
xy		14.22	33.45	8.33	79.70	1.43
yz	1.02	16.51	2.20	13.76	9.20	
zx	1.02	2.89	40.82	7.44	9.20	
S	20.84	2.71	1.66			
P_x			1.83	2.80		
P_y						
P_z		1.78		3.34		1.54

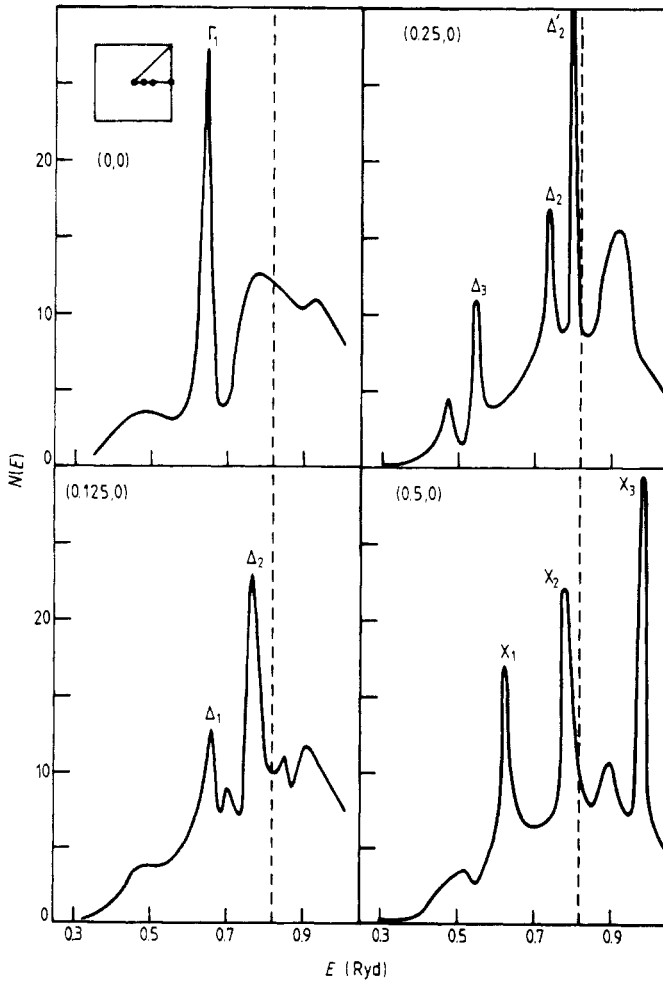


Figure 2. Spectral density of states for the surface plane (100) of Mo along the symmetry line $\bar{\Delta}$ ($\bar{\Gamma}$ - \bar{X} direction of the two-dimensional Brillouin zone).

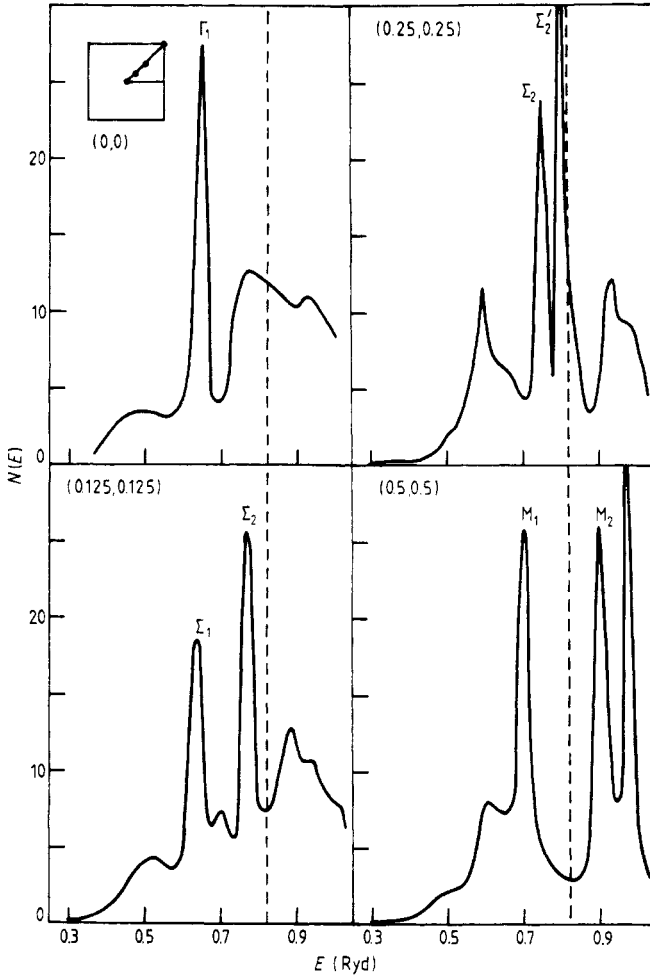


Figure 3. Spectral density of states for the surface plane (100) of Mo along the symmetry line $\bar{\Sigma}$ ($\bar{\Gamma}$ - \bar{M} direction of the two-dimensional Brillouin zone).

plane and end up at X_2 and X_3 . A similar description could be made along the $\bar{\Sigma}$ direction, but we shall not enter into the precise details here. What now concerns us is that this band corresponds to the second low-lying surface band of Weng *et al* (1978). Other surface resonances can be obtained covering several regions of the two-dimensional Brillouin zone, but dwelling on this does not seem useful or especially relevant.

Figure 5 shows, finally, the total density of states on the first four atomic planes. Although we found overall agreement with other calculations (Bertoni *et al* 1977, Inglesfield 1978, Weng *et al* 1978, Kerker *et al* 1978), we did not perform a thorough integration over the two-dimensional Brillouin zone, as required, but used instead the Cunningham (1974) technique, i.e., we took the average of the spectral density of states over a small set of selected points of the two-dimensional Brillouin zone (ten points in our case). Even so, the density of states thus calculated at the surface and fourth atomic planes exhibits the main features of the surface and bulk density of states calculated by other more refined techniques (also more time consuming) of integration over the Brillouin zone.

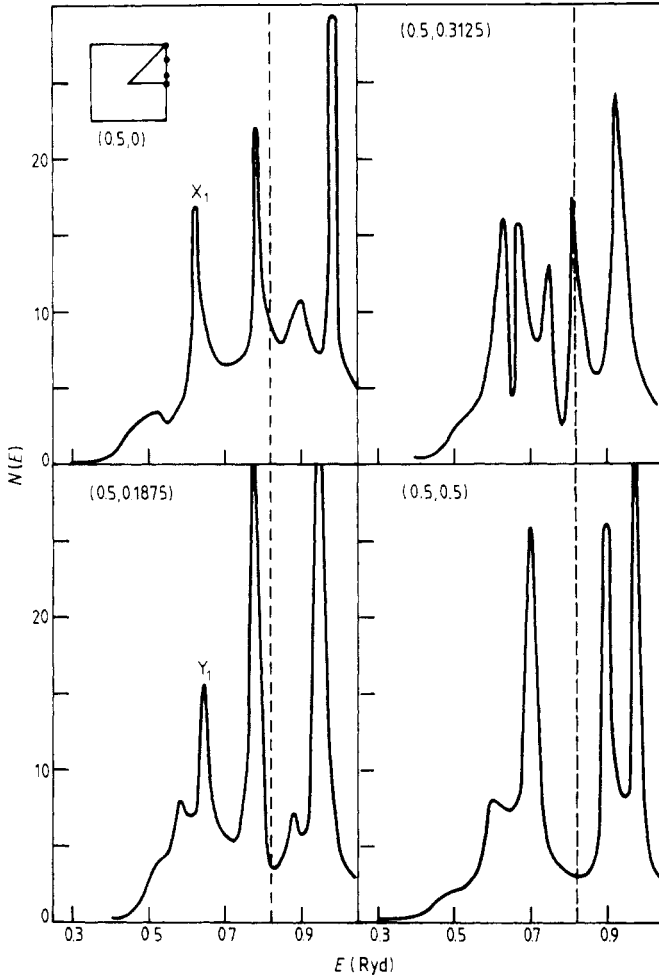


Figure 4. Spectral density of states for the surface plane (100) of Mo along the symmetry line \bar{Y} (\bar{X} - \bar{M} direction of the two-dimensional Brillouin zone).

5. Discussion and concluding remarks

Weng *et al* (1978) carried out a rather thorough photoemission study of the surface states and resonances at the (100) face of two closely similar metals: Mo and W. They found *three* occupied bands of surface resonances, located about 0.2, 0.6 and 3.3 eV below the Fermi level, of main symmetry Δ_1 , Δ_2 and Δ_1 , respectively, along the $\bar{\Delta}$ direction. The first one gives a strong surface-state peak at the point $\bar{\Gamma}$ and falls quickly in intensity as one moves off $\bar{\Gamma}$ (the Swanson hump; Swanson and Crouser 1967). The second one does not exist at the $\bar{\Gamma}$ point and its immediate neighbourhood, and results in a shoulder below the surface-state peak in field emission as well as in integrated photoemission. The third band is made up mainly of dz^2 and s orbitals.

Our calculation gives the second and third bands but fails to reproduce the surface-state peak just below the Fermi level. The high convergence of the iteration scheme given in

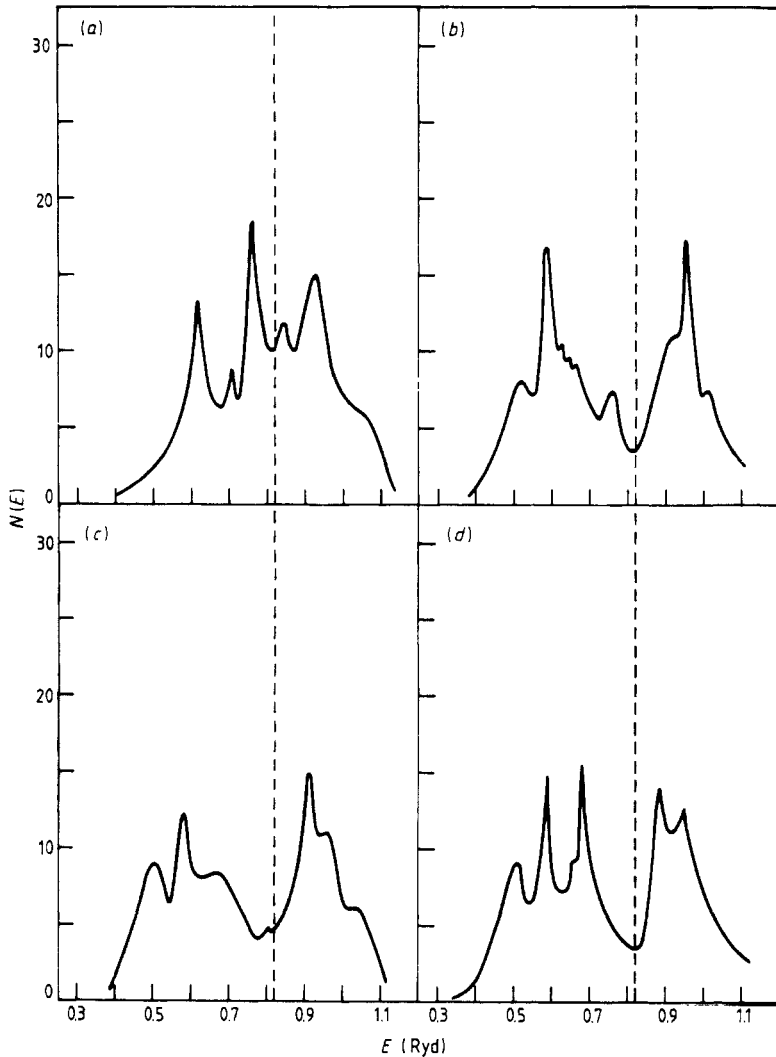


Figure 5. Total densities of states for Mo(100) calculated for (a) the surface, (b) the second layer, (c) the third layer and (d) the fourth layer.

the present paper was used here just to look for this thin peak. The imaginary part of the energy (η) was set equal to 10^{-5} Ryd and the range from 0.75 to 0.90 Ryd was covered at intervals of 10^{-3} Ryd. This can be done with the present method with a small extra cost in computing time as the number of iterations to obtain the T matrix rises from 6 (at $\eta = 10^{-2}$ Ryd) to only 15 at $\eta = 10^{-5}$ Ryd. No trace of any peak, thin or broad, was found in this energy range.

This was only to be expected. The model does not incorporate the appropriate boundary condition at the surface and, consequently, it is unable to reproduce the surface-state peak. All the experience gathered so far through different calculations seems to suggest that the surface band just below the Fermi level is a band of intrinsic, or '*bona fide*' surface states, strongly dependent on choosing an appropriate surface potential. This potential must jump by several eV in a distance of about an interlayer. All the calculations

which have put this discontinuity at the surface obtained the surface-state peak (Kerker *et al* 1978, Inglesfield 1978; those which do not, fail to obtain it (Weng *et al* 1978, Bertoni *et al* 1978). For the closely related case of W (100), we have two calculations rather carefully performed with two different models. While the pseudopotential calculation of Posternak *et al* (1980) obtains the Swanson hump, the tight-binding calculation of Grise *et al* (1979) (overlap included) does not; the same applies to the calculation of Laks and Gonçalves da Silva (1978).

Once the appropriate boundary conditions are used, self-consistency of the surface potential is important in order to place the surface state below the Fermi level. Thus Inglesfield (1978), who used the matching Green function method and therefore had a discontinuous potential at the surface, obtained the surface state above the Fermi level; if the calculation were carried out to the level of self-consistency, the surface state would most probably come down below the Fermi level.

In summary, the Swanson hump seems to be the kind of surface state which comes out naturally with the matching surface Green function method (Garcia-Moliner and Rubio 1969, 1971, Inglesfield 1971). The tight-binding scheme has difficulty because it does not take into account matching to the scattering states of the surface atom, which lie above the vacuum level and are essential to obtain intrinsic surface states. What is really needed is some kind of hybrid between both methods, something which can unite the simplicity of the transfer-matrix technique in describing the bulk with the correct way of imposing surface boundary conditions provided by matching Green functions. This will be attempted in a forthcoming publication.

References

- Ainshchik V, Falicov L M and Yndurain F 1976 *Surf. Sci.* **57** 375–84
 Bertoni C M, Calandra C and Manghi F 1977 *Solid State Commun.* **23** 255–9
 Cunningham S L 1974 *Phys. Rev. B* **10** 4988–94
 Dy K S, Wu Shi-Yu and Sprathn T 1979 *Phys. Rev. B* **20** 4237–43
 Foo E N, Thorpe M F and Weaire D 1976 *Surf. Sci.* **57** 323–47
 Garcia-Moliner F and Rubio J 1969 *J. Phys. C: Solid State Phys.* **2** 1789–96
 ——— 1971 *Proc. R. Soc. A* **324** 257–73
 Grise W R, Dempsey D G, Kleinman L and Madrick K 1979 *Phys. Rev. B* **20** 3045–50
 Haydock R, Heine V and Kelly M J 1972 *J. Phys. C: Solid State Phys.* **5** 2845–58
 ——— 1975 *J. Phys. C: Solid State Phys.* **8** 2591–605
 Inglesfield J E 1971 *J. Phys. C: Solid State Phys.* **4** L14–7
 ——— 1978 *Surf. Sci.* **76** 379–96
 Kerker G P, Ho K M and Cohen M L 1978 *Phys. Rev. Lett.* **40** 1593–6
 Laks B and Gonçalves da Silva C E T 1978 *Solid State Commun.* **25** 401–3
 Lee D H and Joannopoulos J D 1981a *Phys. Rev. B* **23** 4988–96
 ——— 1981b *Phys. Rev. B* **23** 4997–5004
 Mele E J and Joannopoulos J D 1978 *Phys. Rev. B* **17** 1816–27
 Petroff I and Viswanathan C R 1971 *Phys. Rev. B* **4** 799–816
 Posternak M, Krakauer H, Freeman A J and Koelling D D 1980 *Phys. Rev. B* **21** 5601–12
 Slater J C and Koster G F 1954 *Phys. Rev.* **94** 1498–524
 Swanson W and Crouser L C 1967 *Phys. Rev. Lett.* **19** 1179–82
 Weng Shang-Lin, Plummer E W and Gustafsson T 1978 *Phys. Rev. B* **18** 1718–39